J Mol Model (2013) 19:4561–4573
DOI 10.1007/s00894-013-1953-2

ORIGINAL PAPER

2,3′-Diamino-4,4′-stilbenedicarboxylic acid sensitizer for dye-sensitized solar cells: quantum chemical investigations

Palanivel Senthilkumar · Chandrasekaran Nithya · Ponnusamy Munusamy Anbarasan

Received: 1 May 2013 / Accepted: 17 July 2013 / Published online: 20 August 2013

Abstract The metal-free organic dye sensitizer 2,3′-diamino-4,4′-stilbenedicarboxylic acid has been investigated for the first time for dye-sensitized solar cell applications. Density functional theory (DFT) and time-dependent DFT (TD-DFT) calculations (performed using the hybrid functional B3LYP) were carried out to analyze the geometry, electronic structure, polarizability, and hyperpolarizability of 2,3′-diamino-4,4′-stilbenedicarboxylic acid used as a dye sensitizer. A TiO_2 cluster was used as a model semiconductor when attempting to determine the conversion efficiency of the selected dye sensitizer. Our TD-DFT calculations demonstrated that the twenty lowest-energy excited states of 2,3′-diamino-4,4′-stilbenedicarboxylic acid are due to photoinduced electron-transfer processes. Moreover, interfacial electron transfer between a TiO_2 semiconductor electrode and the dye sensitizer occurs through electron injection from the excited dye to the semiconductor's conduction band. Results reveal that metal-free 2,3′-diamino-4,4′-stilbenedicarboxylic acid is a simple and efficient sensitizer for dye-sensitized solar cell applications.

Keywords Dye sensitizer · Density functional theory · Electronic structure · NBO analysis · Absorption spectrum

PACS no 78.66.Qn · 31.10.+z · 71.15.Mb · 32.30

P. Senthilkumar · P. M. Anbarasan (✉)
Department of Physics, Periyar University, Salem 636 011, Tamil Nadu, India
e-mail: anbarasanpm@gmail.com

C. Nithya
Centre for Energy and Environmental Science and Technology, National Institute of Technology, Tiruchirappalli 620 015, Tamil Nadu, India

Introduction

The rapid increase in CO_2 pollution, which has been linked to global warming—a serious threat to the environment, has driven the search for clean and green energy sources in recent decades. Among the most significant of these sources are dye-sensitized solar cells (DSSCs), which were discovered by O'Regan and Gratzel et al. [1] in 1991. Ru-based sensitizers have attracted much attention because they exhibit impressive solar energy conversion efficiencies of ~11.1 % [2–4]. However, the depletion of Ru and its toxicity have prompted research into metal-free organic sensitizers that are inexpensive, abundant, ecofriendly, have high molar absorption coefficients, and, most importantly, have tunable spectral and electrochemical properties [5–8]. The basic architectural unit (Scheme 1) for a sensitizer is donor–spacer–acceptor (or D-S-A), which promotes intramolecular charge transfer (ICT) during photoexcitation. Therefore, the most important strategy for developing such sensitizers is to synthesize high-efficiency organic dyes that harvest all of the photons in the visible and near-IR regions. To increase the efficiency of such a dye, it must have a suitable chromopore with extended π-conjugation that redshifts the absorption spectrum. Although the ethylene unit is commonly used in this context, it exhibits low quantum efficiency due to substantial energy loss upon photoisomerization [9–11]. To overcome this problem, researchers have also considered stilbene (Fig. 1), which has quantum efficiency of 9 % [12], as a sensitizer; however, *cis*/*trans* isomerization is a commonly encountered issue in stilbene derivatives. Therefore, inhibiting the central double bond (i.e., the bond that cause the *cis*/*trans* isomerization) in stilbene derivatives should increase the quantum efficiency of DSSCs. To lock the molecule into the transoid geometry and increase the solar energy conversion efficiency, suitable donor and acceptor moieties must be present

in the stilbene derivative. In the work described in the present paper, we studied a novel potential stilbene-based sensitizer, 2,3′-diamino-4,4′-stilbenedicarboxylic acid, which has a carboxylic acid group as the electron acceptor and an amino group as the electron donor (Fig. 1). The present work represents the first time that this potential sensitizer has been investigated. Carboxylic acids [1, 9, 13] are often employed as electron acceptors, as they possess very good anchoring properties, so they can easily attach to the surface of TiO_2. According to Gratzel [14] and Lin et al. [15], amino groups are notable electron donors, and solar cells that utilize sensitizers with amino groups as donor groups exhibit excellent stability under heating and continuous illumination. For the present work, these donor and acceptor groups were inserted at the 2, 3′ and 4, 4′ positions, respectively, in the stilbene molecule, although other positions are also possible. These particular positions were chosen because placing the substituents at other positions leads to symmetric structures that exhibit poor conversion efficiency. Generally, the structure of the molecule influences its nonlinearity. Molecules with high NLO exhibit large dipole moments in the excited state, which in turn lead to good photoelectric conversion. High NLO requires an asymmetric structure [16, 17]. In this work, we investigated the structural and electronic properties (geometry, natural bond orbitals (NBOs), nonlinear optical (NLO) properties, and the electronic absorption spectrum) of the selected potential dye sensitizer by performing quantum chemical calculations based on density functional theory (DFT) and time-dependent DFT in order to elucidate its sensitizing properties.

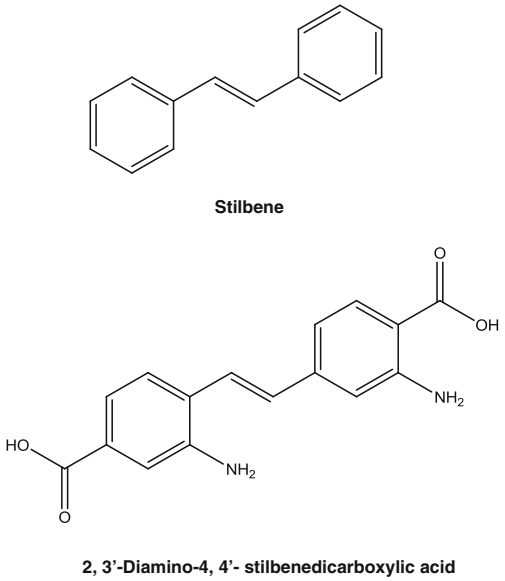

Fig. 1 Structures of stilbene and 2,3′-diamino-4,4′-stilbenedicarboxylic acid

Computational methods

The geometry, electronic structure, polarizability, and hyperpolarizability of the dye 2,3′-diamino-4,4′-stilbenedicarboxylic acid were calculated based on DFT using the Gaussian 09w package [18]. The Becke three-parameter and Lee–Yang–Parr (B3LYP) hybrid functional [19–21] was utilized in the DFT calculations, all of which were performed without any symmetry constraints using polarized triple-zeta 6-311++G(d,p) basis sets. Natural bond orbital (NBO) analysis was performed using restricted Hartree–Fock (RHF) with the 6-311++G(d,p) basis set. The electronic absorption spectrum was derived by calculating the allowed excitations and oscillator strengths. These calculations were done using TD-DFT with the same basis sets and exchange-correlation functional in a vacuum and solution, and the nonequilibrium version of the polarizable continuum model (PCM) [22, 23] was adopted to calculate solvent effects.

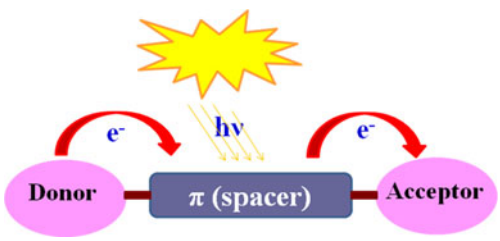

Scheme 1 Structure of the basic architectural unit of the dye sensitizer

Results and discussion

Geometric structure

The geometric structure of 2,3′-diamino-4,4′-stilbenedicarboxylic acid was optimized using HF/6-311++G(d,p) and B3LYP/6-311++G(d,p). The optimized geometry of 2,3′-diamino-4,4′-stilbenedicarboxylic acid is shown in Fig. 2, and the bond lengths, bond angles, and dihedral angles are listed in Table 1. Although the crystal structure of this compound is not yet available, we can compare the optimized structure with other similar systems for which the crystal structures have been solved. Using the optimized geometry, we can find most of the optimized bond lengths, bond angles, and dihedral angles theoretically. The geometrical data reported in the present work are mainly for the donor and acceptor parts of the sensitizer, which are primarily required for practical DSSCs. Therefore, we obtained most of the geometrical data for these parts of the optimized structure.

Electronic structures and charges

To investigate the charge populations of 2,3′-diamino-4,4′-stilbenedicarboxylic acid, we performed NBO analysis of this

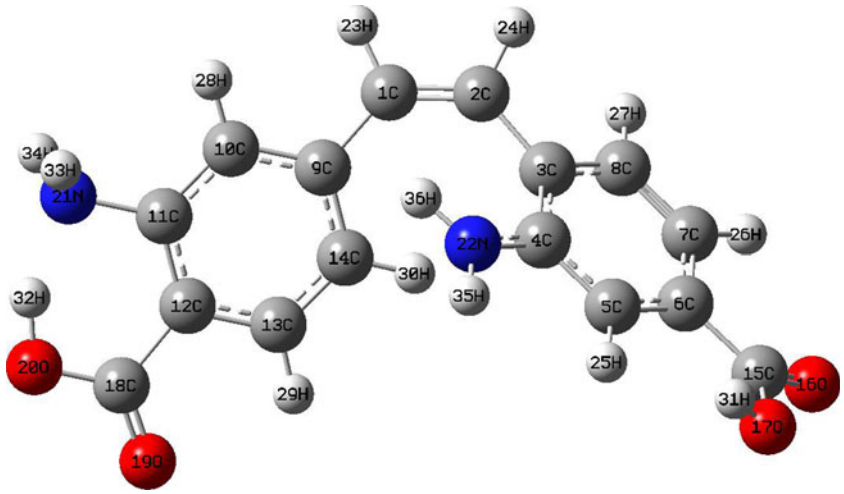

Fig. 2 Optimized geometry of 2,3′-diamino-4,4′-stilbenedicarboxylic acid

dye molecule. The energies of its frontier molecular orbitals (MO) and the corresponding density of state of the dye is shown in Fig. 3. In this work, we used the HF methodology to carry out the NBO analysis because the minimal basis set was sufficient for this analysis. We can also use DFT for analysis, but this requires the use of a higher-level basis set. The HOMO–LUMO gap of the dye 2,3′-diamino-4,4′-stilbenedicarboxylic acid in vacuum is 3.63 eV. In the present work, we used the $Ti_{38}O_{76}$ cluster because it has been shown to be an excellent semiconductor for DSSCs [24], so we used it as a model to understand the properties of DSSCs. While the calculated HOMO and LUMO energies of the bare $Ti_{38}O_{76}$ cluster selected as a nanocrystalline model were −6.55 and −2.77 eV, respectively, and the HOMO–LUMO band gap of the semiconductor was 3.78 eV, the lowest transition was 3.20 eV according to TD-DFT calculations. Given the calculated HOMO (−5.61 eV), LUMO (−1.98 eV), and HOMO–LUMO gap (3.63 eV) of the dye, it is clear that the HOMO energy of the dye fall within the HOMO energy of TiO_2. This is due to interfacial electron transfer [25] between the TiO_2 electrode and the 2,3′-diamino-4,4′-stilbenedicarboxylic acid, which results in electron injection from the excited dye to the semiconductor conduction band.

Polarizability and hyperpolarizability

The optical properties of the dye system greatly influence the photoelectric conversion efficiency, which indicates how the structure of the molecule affects its nonlinearity. This provides valuable information about how these structural differences compete between various molecules (e.g., in DSSC, TiO_2-like semiconductors, etc.). Based on molecular structure analysis, we are able to formulate hypotheses about the optical characteristics of a dye. Delocalized π-electrons that travel along the molecule's conjugated backbone (i.e., its long axis) generate nonlinearity in the molecule. The distance traveled is proportional to the magnitude of the nonlinearity. Therefore, a longer conjugated molecule is more nonlinear, leading to better photoelectric conversion efficiency. Usually, nonlinear optical properties—which require asymmetric structure, leading to a large dipole moment—result in good photoelectric conversion (see Zang et al. [26]). Moreover, a dye sensitizer is characterized by two important physical quantities: the dipole and the polarizability [27].

A system with D-π-A conjugation has high polarizability because this kind of molecular structure promotes intramolecular photoinduced electron transfer between a donor and an acceptor through π-bridges with strong polarity. Such a system may show a considerable photoelectric conversion rate, photorefractive effect, and nonlinear optical effect [28]. On the other hand, charge separation is associated with photocurrent generation and charge dissociation, which also requires a large dipole moment in the excited state. Therefore, it is reasonable to expect that the higher the molecular polarizability, the better the molecular photoelectric conversion efficiency [17].

Further, in order to get a molecule with a large difference between the dipole moment of its ground state and that of its excited state, an asymmetric structure is needed that is a strong donor on one side and a strong acceptor on the other side, with the two sides linked by a spacer with extended conjugation. Such a structure presents a large second-harmonic generation effect, which is, in turn, correlated with nonlinear optics. Photocurrent generation is coupled with charge separation, which also requires a large dipole moment in the excited state. To determine the intramolecular excited states, and the intermolecular charge transfer in exciplexes [29–31], the dipole moment and polarizability must be known.

In order to investigate the above observations, we used B3LYP/6-311++G(d,p) to compute the polarizabilities and hyperpolarizabilities of 2,3′-diamino-4,4′-stilbenedicarboxylic acid so that we could elucidate the relationships between

Table 1 Selected bond lengths (in Å) and bond angles (in degrees) of the dye 2,3′-diamino-4,4′-stilbenedicarboxylic acid

Parameter	HF/6-311++G(d,p)	B3LYP/6-311++G(d,p)
Bond length (Å)		
H(36)–N(22)	0.9943	1.0106
H(35)–N(22)	0.9951	1.0115
H(34)–N(21)	1.008	1.0269
H(33)–N(21)	1.0073	1.0261
H(32)–O(20)	0.9865	1.0503
H(31)–O(17)	0.9637	0.9924
H(30)–C(14)	1.0676	1.081
H(29)–C(13)	1.0697	1.0829
H(28)–C(10)	1.0734	1.0858
H(27)–C(8)	1.0725	1.0846
H(26)–C(7)	1.0693	1.0813
H(25)–C(5)	1.072	1.0854
H(24)–C(2)	1.0765	1.0897
H(23)–C(1)	1.0758	1.0886
N(22)–C(4)	1.3703	1.3673
N(21)–C(11)	1.4557	1.4716
O(20)–C(18)	1.3345	1.3503
O(19)–C(18)	1.2048	1.231
C(18)–C(12)	1.5075	1.5177
O(17)–C(15)	1.3628	1.3878
O(16)–C(15)	1.1985	1.2228
C(15)–C(6)	1.4902	1.4937
C(14)–C(13)	1.3764	1.4108
C(14)–C(9)	1.3919	1.3868
C(13)–C(12)	1.3862	1.3985
C(12)–C(11)	1.388	1.4021
C(11)–C(10)	1.3828	1.3924
C(10)–C(9)	1.39	1.4084
C(9)–C(1)	1.4803	1.4705
C(8)–C(3)	1.3865	1.3857
C(8)–C(7)	1.3792	1.4072
C(7)–C(6)	1.3812	1.3995
C(6)–C(5)	1.3802	1.3914
C(5)–C(4)	1.3943	1.4114
C(4)–C(3)	1.4033	1.4274
C(3)–C(2)	1.4895	1.4773
C(2)–C(1)	1.3249	1.3513
Bond angle (°)		
C(4)–N(22)–H(35)	120.5931	120.7782
C(4)–N(22)–H(36)	120.4116	120.4927
H(35)–N(22)–H(36)	118.126	118.5482
C(11)–N(21)–H(33)	113.3067	112.5442
C(11)–N(21)–H(34)	113.0799	112.2351
H(33)–N(21)–H(34)	110.8388	109.749
C(18)–O(20)–H(32)	111.9976	108.1873
C(12)–C(18)–O(19)	120.9445	120.7161
C(12)–C(18)–O(20)	116.8609	115.8845
O(19)–C(18)–O(20)	122.1937	123.3976
C(15)–O(17)–H(31)	114.7709	111.1255
C(6)–C(15)–O(16)	123.4921	123.6806
C(6)–C(15)–O(17)	116.231	116.4122
O(16)–C(15)–O(17)	120.2748	119.9055
H(30)–C(14)–C(13)	119.9521	119.3012
H(30)–C(14)–C(9)	120.0235	120.3723
C(13)–C(14)–C(9)	120.0231	120.3151
H(29)–C(13)–C(14)	120.896	121.8473
H(29)–C(13)–C(12)	117.594	116.6949
C(14)–C(13)–C(12)	121.5099	121.4578
C(18)–C(12)–C(13)	115.8769	116.2468
C(18)–C(12)–C(11)	125.1938	124.9889
C(13)–C(12)–C(11)	118.9292	118.7642
N(21)–C(11)–C(12)	120.1792	118.6534
N(21)–C(11)–C(10)	120.3177	121.3261
C(12)–C(11)–C(10)	119.5024	120.0201
H(28)–C(10)–C(11)	118.7855	119.3516
H(28)–C(10)–C(9)	119.4843	119.1914
C(11)–C(10)–C(9)	121.73	121.4567
C(1)–C(9)–C(14)	123.6874	123.6829
C(1)–C(9)–C(10)	117.9996	118.3058
C(14)–C(9)–C(10)	118.2907	117.9695
H(27)–C(8)–C(3)	118.5956	119.8014
H(27)–C(8)–C(7)	119.7467	118.0508
C(3)–C(8)–C(7)	121.6552	122.1373
H(26)–C(7)–C(8)	121.7965	122.3158
H(26)–C(7)–C(6)	119.559	118.7493
C(8)–C(7)–C(6)	118.6442	118.9343
C(15)–C(6)–C(7)	117.7168	117.0469
C(15)–C(6)–C(5)	121.6136	122.6778
C(7)–C(6)–C(5)	120.6536	120.2599
H(25)–C(5)–C(6)	120.2637	120.2881
H(25)–C(5)–C(4)	118.4192	117.963
C(6)–C(5)–C(4)	121.2627	121.6848
N(22)–C(4)–C(5)	120.4746	120.321
N(22)–C(4)–C(3)	121.5568	121.7477
C(5)–C(4)–C(3)	117.9684	117.9306
C(2)–C(3)–C(8)	118.8939	117.8267
C(2)–C(3)–C(4)	121.2656	122.9798
C(8)–C(3)–C(4)	119.7976	119.0109
H(24)–C(2)–C(1)	117.1253	115.3581
H(24)–C(2)–C(3)	114.42	113.0107
C(1)–C(2)–C(3)	128.4533	131.628
H(23)–C(1)–C(2)	116.9538	115.885
H(23)–C(1)–C(9)	113.8114	113.4291
C(2)–C(1)–C(9)	129.2345	130.6159

Table 1 (continued)

Parameter	HF/6-311++G(d,p)	B3LYP/6-311++G(d,p)
Dihedral angle (°)		
H(36)–N(22)–C(4)–C(3)	5.5522	3.1547
H(36)–N(22)–C(4)–C(5)	−174.596	−177.164
H(35)–N(22)–C(4)–C(3)	174.6797	178.1961
H(35)–N(22)–C(4)–C(5)	−5.4681	−2.1222
H(34)–N(21)–C(11)–C(10)	67.6402	66.7868
H(34)–N(21)–C(11)–C(12)	−112.069	−112.972
H(33)–N(21)–C(11)–C(10)	−59.5615	−57.6121
H(33)–N(21)–C(11)–C(12)	120.7295	122.629
H(32)–O(20)–C(18)–O(19)	−179.994	−179.98
H(32)–O(20)–C(18)–C(12)	0.352	0.5012
O(20)–C(18)–C(12)–C(11)	−1.0335	−0.8053
O(20)–C(18)–C(12)–C(13)	179.0682	179.045
O(19)–C(18)–C(12)–C(11)	179.3077	179.662
O(19)–C(18)–C(12)–C(13)	−0.5906	−0.4876
H(31)–O(17)–C(15)–O(16)	156.0592	162.4026
H(31)–O(17)–C(15)–C(6)	−23.4334	−17.1396
O(17)–C(15)–C(6)–C(5)	−19.7877	−17.1532
O(17)–C(15)–C(6)–C(7)	161.6609	164.2745
O(16)–C(15)–C(6)–C(5)	160.7378	163.3237
O(16)–C(15)–C(6)–C(7)	−17.8136	−15.2486
C(9)–C(14)–C(13)–C(12)	0.1002	−0.9804
C(9)–C(14)–C(13)–H(29)	179.9688	−178.584
H(30)–C(14)–C(13)–C(12)	−179.486	177.7946
H(30)–C(14)–C(13)–H(29)	0.3823	0.1914
C(13)–C(14)–C(9)–C(10)	−1.0989	−0.1357
C(13)–C(14)–C(9)–C(1)	−179.342	179.8024
H(30)–C(14)–C(9)–C(10)	178.4873	−178.897
H(30)–C(14)–C(9)–C(1)	0.244	1.0407
C(14)–C(13)–C(12)–C(11)	0.7913	1.0763
C(14)–C(13)–C(12)–C(18)	−179.304	−178.784
H(29)–C(13)–C(12)–C(11)	−179.081	−178.865
H(29)–C(13)–C(12)–C(18)	0.8236	1.275
C(13)–C(12)–C(11)–C(10)	−0.6548	−0.877
C(13)–C(12)–C(11)–N(21)	179.0566	178.8851
C(18)–C(12)–C(11)–C(10)	179.4498	178.9699
C(18)–C(12)–C(11)–N(21)	−0.8389	−1.268
C(12)–C(11)–C(10)–C(9)	−0.3652	−0.2525
C(12)–C(11)–C(10)–H(28)	179.5057	179.5517
N(21)–C(11)–C(10)–C(9)	179.9239	179.9919
N(21)–C(11)–C(10)–H(28)	−0.2052	−0.2039
C(11)–C(10)–C(9)–C(14)	1.2418	1.1779
C(11)–C(10)–C(9)–C(1)	179.5863	178.9127
H(28)–C(10)–C(9)–C(14)	−178.628	−178.627
H(28)–C(10)–C(9)–C(1)	−0.2837	−0.8918
C(10)–C(9)–C(1)–C(2)	156.6363	166.2351
C(10)–C(9)–C(1)–H(23)	−23.1755	−16.9852
C(14)–C(9)–C(1)–C(2)	−25.1156	−16.1692
C(14)–C(9)–C(1)–H(23)	155.0725	160.6105
C(7)–C(8)–C(3)–C(4)	0.5439	−2.2572
C(7)–C(8)–C(3)–C(2)	178.1916	178.021
H(27)–C(8)–C(3)–C(4)	179.9663	178.9433
H(27)–C(8)–C(3)–C(2)	−2.386	−0.7785
C(3)–C(8)–C(7)–C(6)	−1.4514	2.1868
C(3)–C(8)–C(7)–H(26)	178.7468	177.4232
H(27)–C(8)–C(7)–C(6)	179.1328	−178.994
H(27)–C(8)–C(7)–H(26)	−0.6691	−3.7572
C(8)–C(7)–C(6)–C(5)	1.6041	1.5885
C(8)–C(7)–C(6)–C(15)	−179.83	−179.803
H(26)–C(7)–C(6)–C(5)	−178.59	−178.68
H(26)–C(7)–C(6)–C(15)	−0.0236	−0.071
C(7)–C(6)–C(5)–C(4)	−0.871	−0.9201
C(7)–C(6)–C(5)–H(25)	176.4036	176.1086
C(15)–C(6)–C(5)–C(4)	−179.38	−179.448
C(15)–C(6)–C(5)–H(25)	−2.1058	−2.4192
C(6)–C(5)–C(4)–C(3)	−0.0584	0.8283
C(6)–C(5)–C(4)–N(22)	−179.916	−178.865
H(25)–C(5)–C(4)–C(3)	−177.382	−176.267
H(25)–C(5)–C(4)–N(22)	2.7608	4.0394
C(5)–C(4)–C(3)–C(8)	0.2222	−1.4142
C(5)–C(4)–C(3)–C(2)	−177.368	−176.392
N(22)–C(4)–C(3)–C(8)	−179.922	178.2748
N(22)–C(4)–C(3)–C(2)	2.4873	3.2974
C(4)–C(3)–C(2)–C(1)	−68.9079	−49.4194
C(4)–C(3)–C(2)–H(24)	111.5539	131.277
C(8)–C(3)–C(2)–C(1)	113.4802	135.5472
C(8)–C(3)–C(2)–H(24)	−66.0579	−43.7564
C(3)–C(2)–C(1)–C(9)	−0.9971	−6.9436
C(3)–C(2)–C(1)–H(23)	178.8098	176.3407
H(24)–C(2)–C(1)–C(9)	178.5305	172.3469
H(24)–C(2)–C(1)–H(23)	−1.6626	−4.3687

photocurrent generation, molecular structure, and NLO for this dye. The relation [27, 32] for the isotropic polarizability is as follows:

$$\alpha = \frac{1}{3}(\alpha_{XX} + \alpha_{YY} + \alpha_{ZZ}). \quad (1)$$

The polarizability anisotropy invariant is

$$\Delta\alpha = \left[\frac{(\alpha_{XX}-\alpha_{YY})^2 + (\alpha_{YY}-\alpha_{ZZ})^2 + (\alpha_{ZZ}-\alpha_{XX})^2}{2}\right]^{\frac{1}{2}}, \quad (2)$$

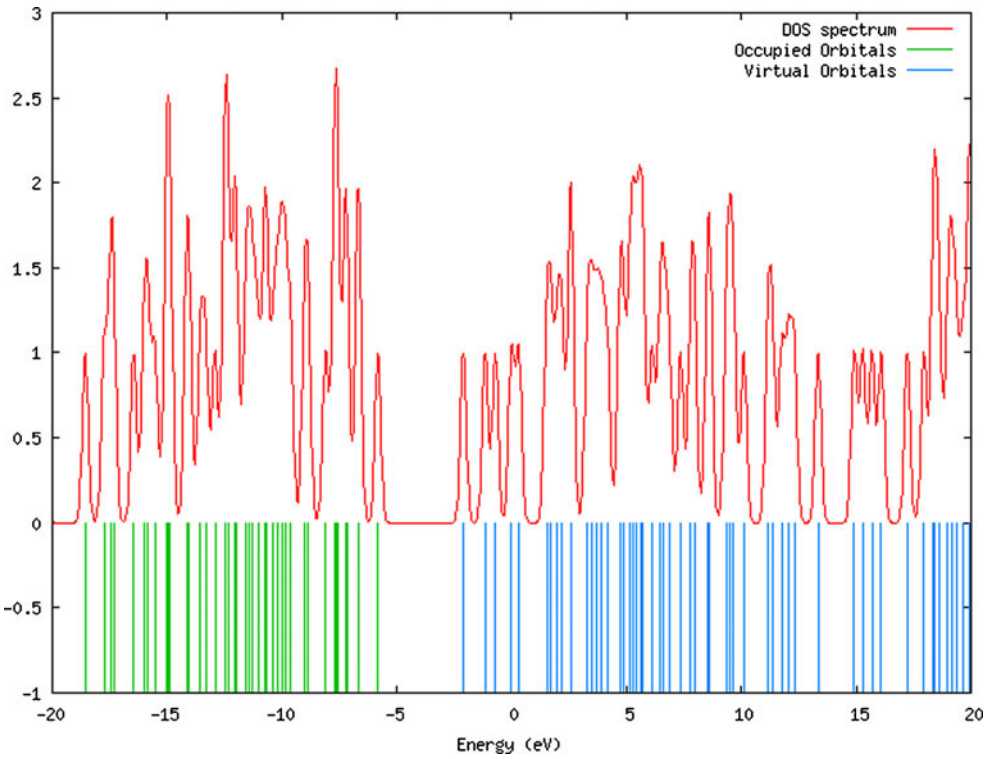

Fig. 3 Frontier molecular orbital energies and corresponding density-of-state (DOS) spectrum of 2,3′-diamino-4,4′-stilbenedicarboxylic acid

and the average hyperpolarizability is

$$\beta = \left(\beta_x + \beta_y + \beta_z\right)^{\frac{1}{2}} \tag{3}$$

$$\beta_x = \beta_{xxx} + \beta_{xyy} + \beta_{xzz}$$
$$\beta_y = \beta_{yyy} + \beta_{xxy} + \beta_{yzz}$$
$$\beta_z = \beta_{zzz} + \beta_{xxz} + \beta_{yyz}.$$

where α_{XX}, α_{YY}, and α_{ZZ} are the tensor components of polarizability and β_{xxx}, β_{xyy}, β_{xzz}, β_{yyy}, β_{xxy}, β_{yzz}, β_{zzz}, β_{xxz}, and β_{yyz} are the tensor components of hyperpolarizability.

Tables 2 and 3 present the values for the isotropic polarizability and hyperpolarizability of the dye 2,3′-diamino-4,4′-stilbenedicarboxylic acid, as well as values for the components of the polarizability and hyperpolarizability. The calculated values for the isotropic polarizability and hyperpolarizability of 2,3′-diamino-4,4′-stilbenedicarboxylic acid are 138.43 and 372.4 a.u., respectively, and the dipole moment difference between the ground and excited state is 2.96 D. As compared to hemicyanine dyes [31], 2,3′-diamino-4,4′-stilbenedicarboxylic acid exhibits better upward band edge displacement (see Zhu et al. [33]). Further, the increased dipole moment of the excited state as compared to the ground state indicates that sizable charge transfer occurs during photoexcitation. The difference between the dipole moment of the excited state and that of the ground state of 2,3′-diamino-4,4′-stilbenedicarboxylic acid is comparable to the corresponding differences for coumarin dyes [34]. This large difference in dipole moment occurs because charge from the region with maximum electron density (the NH_2 group) travels along the π-conjugated backbone until it reaches the carboxylic group substituents upon photoexcitation. A molecule with a large dipole moment and high molecular polarizability would be expected to exhibit a high photoelectric conversion efficiency. Further, structural asymmetry leads to nonlinearity [35]; in other words, this dye molecule, which has a strong donor (amino) group on one side and a strong acceptor (carboxylic acid) group on the other, with both sides linked by a π-bridge, possesses a large dipole moment (6.8030 D) in the excited state, leading to photocurrent generation. This is linked to the charge separation process. The difference (ΔE_R) between the energy level of the edge of the conduction band of TiO_2 and the HOMO of the dye sensitizer is 2.84 eV. This confirms that the charge recombination kinetics are quite sluggish in the excited state (see Wang et al. [36]). Therefore, we

Table 2 Polarizability (α) of the dye 2,3′-diamino-4,4′-stilbenedicarboxylic acid (in a.u.)

	α_{xx}	α_{xy}	α_{yy}	α_{xz}	α_{yz}	α_{zz}	α	$\Delta\alpha$
HF/6-311++G(d,p)	−152.09	−16.23	−145.43	−2.85	4.23	−117.77	138.43	31.51
DFT/6-311++G(d,p)	−157.05	−21.40	−135.50	1.37	−7.09	−118.92	137.15	33.21

Table 3 Hyperpolarizability (β) of the dye 2,3′-diamino-4,4′-stilbenedicarboxylic acid (in a.u.)

	β_{xxx}	β_{xxy}	β_{xyy}	β_{yyy}	β_{xxz}	β_{xyz}	β_{yyz}	β_{xzz}	β_{yzz}	β_{zzz}	β
HF/6-311++G(d,p)	185.90	−254.45	2.41	−81.72	73.86	−24.40	8.52	−10.50	6.10	43.07	372.24 (3.215×10^{-30} esu)
DFT/6-311++G(d,p)	−249.22	250.34	13.57	58.98	82.01	−24.81	11.16	1.30	−15.99	33.17	396.13 (3.422×10^{-30} esu)

expect that applying 2,3′-diamino-4,4′-stilbenedicarboxylic acid as a dye sensitizer in DSSCs would lead to reduced dye recombination in the excited state during photoexcitation.

FT-IR and FT-Raman spectra

Figures 4 and 5 show the calculated IR and Raman spectra of 2,3′-diamino-4,4′-stilbenedicarboxylic acid, respectively. Calculated IR and Raman spectra were plotted using a pure Lorentzian band shape with a bandwidth (FWHM) of 10 cm^{-1}. These calculations were done using HF/B3LYP/6-311++G(d,p) and DFT/B3LYP/6-311++G(d,p). A corrective vibrational scaling factor of 0.9613 [37, 38] for the B3LYP-calculated frequencies or of 0.8982 [31, 32] for the HF-calculated frequencies was applied to account for anharmonicity. Table 4 presents the main characteristics of the HF/6-311++ G(d,p)- and DFT/B3LYP/6-311++G(d,p)-calculated vibrational wavenumbers of 2,3′-diamino-4,4′-stilbenedicarboxylic acid. According to Meic et al., the free *trans*-stilbene molecule shows 72 normal vibrations with a point group of C_{2h}. Generally, 30 phenyl–C vibrations are observed for an isolated phenyl–C, among which 21 modes are in the plane of the benzene ring and 9 modes are out-of-plane. Two phenyl rings are connected through an H–C=C–H bridge, which also shows 30 in-phase and 30 out-of-phase vibrations [39]. In the present work, the calculated IR wavenumbers suggest that 2,3′-diamino-4,4′-stilbenedicarboxylic acid presents 1 C–O torsional, 1 skeletal deformation, 7 ring-deformation, 1 ring-breathing, 8 C–H deformation, 2 C–C stretching, 1 ring-stretching, 6 C=C stretching, 1 each of C–C, O–H, N–H, C=O, and C–O stretching modes, and 1 C–C–C bending vibration mode. As per the selection rule for the C_{2h} point group, A_g and B_g

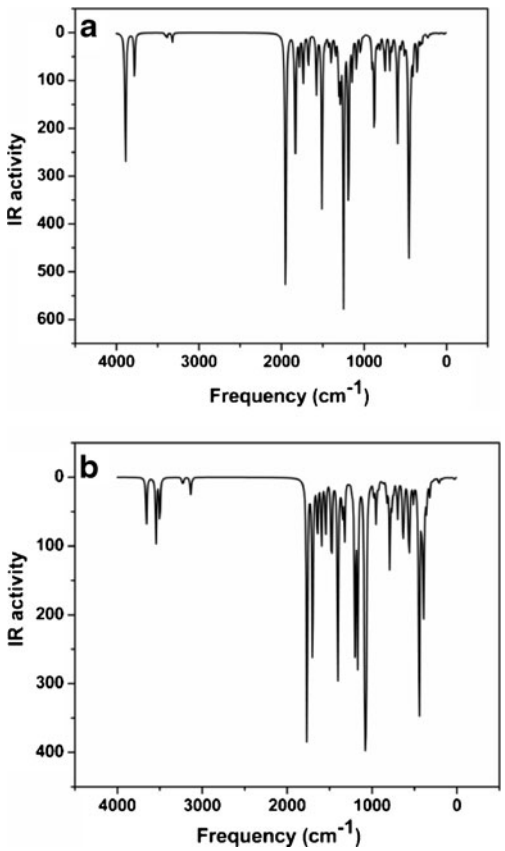

Fig. 4 **a**–**b** FT-IR spectra of 2,3′-diamino-4,4′-stilbenedicarboxylic acid calculated using **a** HF/B3LYP/6-311++G(d,p) and **b** DFT/B3LYP/6-311++G(d,p)

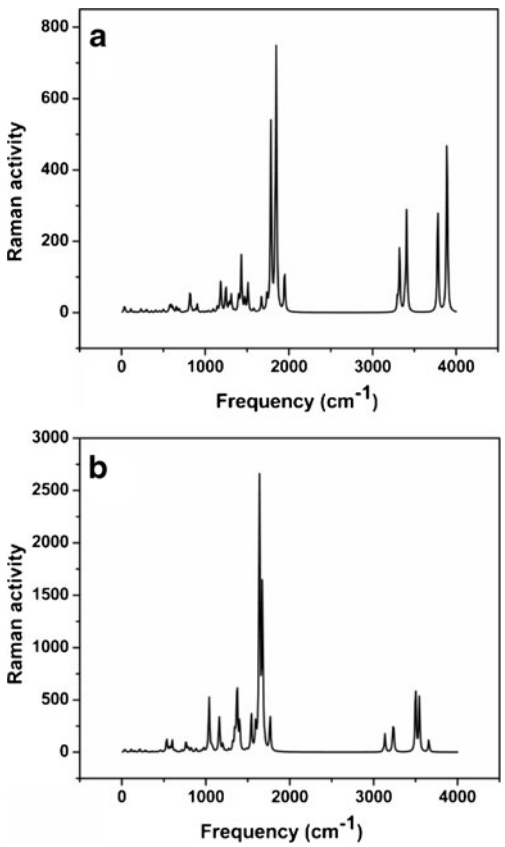

Fig. 5 **a**–**b** FT-Raman spectra of 2,3′-diamino-4,4′-stilbenedicarboxylic acid calculated using **a** HF/B3LYP/6-311++G(d,p) and **b** DFT/B3LYP/6-311++G(d,p)

Table 4 Main characteristics of the vibrational modes of 2,3′-diamino-4,4′-stilbenedicarboxylic acid calculated using HF/B3LYP/6-311++G (d,p) or DFT/B3LYP/6-311++G (d,p)

Vibrational mode no.	Calculated wavenumbers (cm^{-1})				Assignment
	HF/6-311++G(d,p)		DFT/B3LYP/6-311++G(d,p)		
	Wavenumber	IR intensity	Wavenumber	IR intensity	
1	105.27	0.12	103.84	26.73	C–O torsion
2	226.63	6.29	206.44	3.95	Skeletal deformation
3	262.68	0.46	246.54	0.59	Ring deformation
4	348.79	72.42	343.17	12.42	
5	411.59	12.63	397.98	25.41	
6	545.56	21.28	504.04	29.51	
7	610.04	13.04	567.94	16.12	
8	680.44	52.80	627.81	62.65	
9	684.67	0.12	633.11	18.61	
10	833.30	18.99	760.91	26.74	Ring breath
11	740.02	81.33	689.49	54.84	C–H deformation
12	759.58	19.73	707.60	8.35	
13	959.02	0.06	861.21	4.33	
14	1032.56	9.87	944.86	15.30	
15	1165.29	0.34	1032.89	0.006	
16	1177.79	4.71	1063.79	6.880	
17	1183.26	374.22	1077.18	22.91	
18	1300.01	102.07	1229.95	10.132	
19	1025.43	5.602	917.09	15.30	
20	1578.57	11.23	1480.29	21.66	C–C stretching
21	1341.81	41.60	1316.35	88.72	Ring stretching
22	1278.28	14.17	1193.00	20.62	C–O stretching
23	1780.75	16.33	1634.40	21.21	C=O stretching
24	3925.69	0.16	3112.22	1.711	O–H stretching
25	3408.86	0.85	3239.39	0.349	N–H stretching
26	1137.89	0.74	1013.03	1.38	C–C–C bending
27	1425.95	20.21	1357.83	5.53	C=C stretching
28	1461.92	6.00	1358.17	0.44	
29	1469.92	0.69	1367.28	0.10	
30	1504.46	248.09	1395.85	211.81	
31	1506.05	144.40	1397.77	96.03	
32	1571.01	71.26	1469.71	46.42	

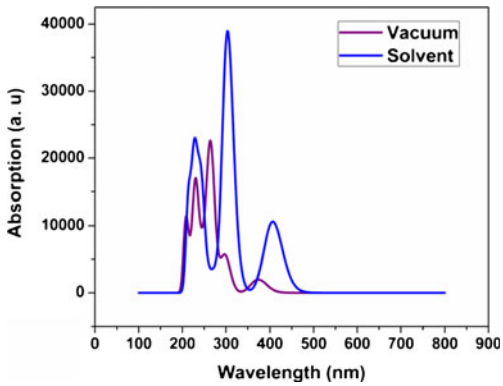

Fig. 6 UV/Vis electronic absorption spectra of 2,3′-diamino-4,4′-stilbenedicarboxylic acid

are in-phase modes that are Raman active, whereas A_u and B_u are out-of phase modes that are IR active. The bands in the calculated Raman spectra (Fig. 4) observed at around 1210, 1595, 1671, 1790, and 3400 cm^{-1} correspond to C–O stretching, NH_2 bending, asymmetric phenyl stretching, ring stretching, and NH_2 stretching vibrations, respectively [40]. According to Baranovic et al. [41], the torsional and out-of-phase modes are very important for photoisomerization. The intense Raman bands correspond to nuclear coordinates at which the excited-state molecules distort very rapidly during photoisomerization. The results obtained suggest that the selected dye architectural unit should exhibit good quantum efficiency upon photoisomerization.

Table 5 Computed excitation energies, electronic transition configurations, and oscillator strengths (*f*, for optical transitions with $f>0.01$) of the absorption bands in the visible and near-UV region for the dye 2,3′-diamino-4,4′-stilbenedicarboxylic acid in acetonitrile solvent

State	Configuration composition (corresponding transition orbitals)	Energy (eV)	Wavelength (nm)	Oscillator strength (*f*)	Major contributors	Minor contributors
1	0.70151 (78→79)	3.0540	405.9703	0.1468	HOMO→LUMO (98 %)	–
2	0.21063 (77→79) 0.66460 (78→80)	3.9148	316.7041	0.0827	HOMO→L+1 (88 %)	H-1→LUMO (9 %)
3	0.65755 (77→79) −0.19376 (78→80)	4.1020	302.2509	0.4932	H-1→LUMO (86 %)	HOMO→L+1 (−8 %)
4	0.64974 (76→79) −0.23698 (76→80) 0.12600 (76→83)	4.2648	290.7131	0.0012	H-2→LUMO (84 %), H-2→L+1 (−11 %)	H-2→L+4 (3 %)
5	0.25645 (75→79) 0.10251 (77→81) 0.64247 (78→81)	4.5120	274.7858	0.0311	H-3→LUMO (13 %), HOMO→L+2 (83 %)	H-1→L+2 (2 %)
6	0.34234 (72→79) 0.22665 (72→80) −0.32833 (73→79) −0.21947 (73→80) 0.34543 (74→79) 0.15162 (74→80)	4.6099	268.9502	0.004	H-6→LUMO (23 %), H-6→L+1 (10 %), H-5→LUMO (−22 %), H-5→L+1 (−10 %), H-4→LUMO (24 %)	H-4→L+1 (5 %)
7	0.18595 (73→79) 0.14572 (74→79) 0.54075 (75→79) 0.19616 (77→80) 0.17562 (77→81) −0.24032 (78→81)	4.6812	264.8537	0.002	H-3→LUMO (58 %), HOMO→L+2 (−12 %)	H-5→LUMO (7 %), H-4→LUMO (4 %), H-1→L+1 (8 %), H-1→L+2 (6 %)
8	0.27631 (73→79) 0.36208 (74→79) −0.21546 (75→79) 0.39389 (77→80) −0.18330 (77→81) 0.14408 (78→81)	4.7645	260.2232	0.0086	H-5→LUMO (15 %), H-4→LUMO (26 %), H-1→L+1 (31 %)	H-3→LUMO (−9 %), H-1→L+2 (−7 %), HOMO→L+2 (4 %)
9	0.35256 (72→79) 0.41909 (73→79) −0.12521 (73→80) −0.38624 (77→80)	4.7977	258.4224	0.0146	H-6→LUMO (25 %), H-5→LUMO (35 %), H-1→L+1 (−30 %)	H-5→L+1 (−3 %)
10	−0.34081 (72→79) 0.35565 (74→79) 0.10713 (77→79) −0.28509 (77→80) −0.34325 (78→82)	5.0934	243.4196	0.2041	H-6→LUMO (−23 %), H-4→LUMO (25 %), H-1→L+1 (−16 %), HOMO→L+3 (−24 %)	H-1→LUMO (2 %)
11	0.63536 (71→79) −0.10419 (72→79) −0.13053 (75→79) 0.15689 (77→81) −0.10192 (78→83)	5.2779	234.9104	0.0062	H-7→LUMO (81 %)	H-6→LUMO (−2 %), H-3→LUMO (−3 %), H-1→L+2 (5 %), HOMO→L+4 (−2 %)
12	0.11674 (74→79) 0.10448 (76→79) 0.22991 (76→80) −0.13429 (77→80) 0.21773 (78→82) 0.56827 (78→83)	5.3334	232.4659	0.0735	H-2→L+1 (11 %), HOMO→L+4 (65 %)	H-4→LUMO (3 %), H-2→LUMO (2 %), H-1→L+1 (−4 %), HOMO→L+3 (9 %)
13	0.24379 (76→79) 0.58844 (76→80) −0.13583 (76→83) −0.21435 (78→83)	5.3515	231.6796	0.0141	H-2→LUMO (12 %), H-2→L+1 (69 %)	H-2→L+4 (−4 %), HOMO→L+4 (−9 %)
14	−0.16048 (71→79) 0.10734 (74→80) −0.22681 (75→79) −0.36246 (75→80) 0.41955 (77→81) −0.20575 (78→82) 0.16849 (78→83)	5.4518	227.4173	0.1074	H-3→LUMO (−10 %), H-3→L+1 (−26 %), H-1→L+2 (35 %)	H-7→LUMO (−5 %), H-4→L+1 (2 %), HOMO→L+3 (−8 %), HOMO→L+4 (6 %)

Table 5 (continued)

State	Configuration composition (corresponding transition orbitals)	Energy (eV)	Wavelength (nm)	Oscillator strength (*f*)	Major contributors	Minor contributors
15	−0.11962 (71→79) −0.11064 (73→79) 0.13883 (73→80) 0.18960 (74→79) −0.25112 (74→80) −0.25013 (75→80) −0.14516 (77→80) 0.11641 (77→81) 0.13722 (77→82) 0.39476 (78→82) −0.24301 (78→83)	5.4803	226.2346	0.0749	H-4→L+1 (−13 %), H-3→L+1 (−13 %), HOMO→L+3 (31 %), HOMO→L+4 (−12 %)	H-7→LUMO (−3 %), H-5→LUMO (−2 %), H-5→L+1 (4 %), H-4→LUMO (7 %), H-1→L+1 (−4 %), H-1→L+2 (3 %), H-1→L+3 (4 %)
16	−0.12722 (71→79) −0.29671 (72→79) 0.33461 (72→80) 0.20516 (73→79) −0.29127 (73→80) 0.26701 (74→80) 0.17498 (78→82)	5.5607	222.9635	0.0438	H-6→LUMO (−18 %), H-6→L+1 (22 %), H-5→L+1 (−17 %), H-4→L+1 (14 %)	H-7→LUMO (−3 %), H-5→LUMO (8 %), HOMO→L+3 (6 %)
17	0.10195 (72→79) 0.15017 (72→80) 0.13972 (73→79) 0.43318 (73→80) 0.13848 (73→81) 0.10519 (74→79) 0.29122 (74→80) 0.27274 (75→80) 0.14100 (77→81)	5.7526	215.5257	0.0055	H-5→L+1 (38 %), H-4→L+1 (17 %), H-3→L+1 (15 %)	H-6→LUMO (2 %), H-6→L+1 (5 %), H-5→LUMO (4 %), H-5→L+2 (4 %), H-4→LUMO (2 %), H-1→L+2 (4 %)
18	0.12762 (72→80) −0.16870 (73→80) −0.28326 (74→80) −0.16013 (74→81) 0.38068 (75→80) −0.17027 (76→81) 0.36088 (77→81)	5.8031	213.6502	0.1504	H-4→L+1 (−16 %), H-3→L+1 (29 %), H-1→L+2 (26 %)	H-6→L+1 (3 %), H-5→L+1 (−6 %), H-4→L+2 (−5 %), H-2→L+2 (−6 %)
19	0.67058 (76→81)	5.8437	212.1658	0.0182	H-2→L+2 (90 %)	
20	−0.13937 (68→79) 0.48255 (70→79) −0.26880 (72→80) −0.11378 (74→81) 0.12067 (76→81) 0.15079 (77→81) −0.21943 (77→82) 0.13492 (78→82)	5.8689	211.2548	0.0118	H-8→LUMO (47 %), H-6→L+1 (−14 %), H-1→L+3 (−10 %)	H-10→LUMO (−4 %), H-4→L+2 (−3 %), H-2→L+2 (3 %), H-1→L+2 (5 %) HOMO→L+3 (4 %)

Electronic absorption spectra and sensitized mechanism

Figure 6 depicts the calculated electronic absorption spectra of 2,3′-diamino-4,4′-stilbenedicarboxylic acid in vacuum and solvent, as determined using TD-DFT(B3LYP)/6-311++G(d,p) calculations. These show three major absorption bands at 405, 301, and 226 nm in solvent and five absorption bands at 374, 295, 262, 228, and 208 nm in vacuum, respectively. As compared to the bands calculated for the molecule in vacuum, the absorption bands of 2,3′-diamino-4,4′-stilbenedicarboxylic acid in solvent are stronger and slightly redshifted, which is due to solvent effects. This can be attributed to the fact that polar solvents usually stabilize or destabilize the molecular orbitals of a compound in the ground state or excited state. The absorption bands at around 208 and 295 nm correspond to π–π* transitions of *trans*-stilbene; however, these bands did not appear separately in solvent, which can be attributed to solvent effects. A band at 228 (in vacuum) or 226 nm (in solvent) is due to a π–π* transition of the carboxylic acid group. The n–π* transition of the carboxylic acid group of the stilbene is observed at around 301 (solvent) or 262 nm (vacuum). A band at around 405 (in solvent) or 374 (in vacuum) is due to intramolecular charge transfer from the amino

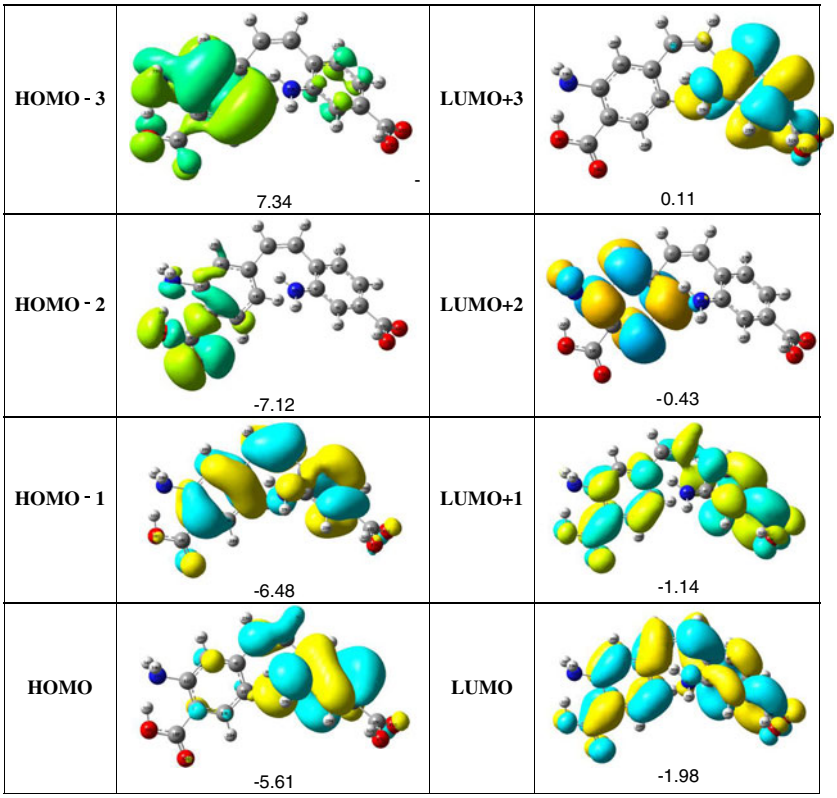

Fig. 7 Isodensity plot (isodensity contour=0.02 a.u.) of the frontier orbitals of 2,3′-diamino-4,4′-stilbenedicarboxylic acid, and the corresponding orbital energies (in eV)

group to the carboxylic acid group; this band is strongly redshifted in solvent. This phenomenon may occur because the electron-withdrawing ability of the carboxylic acid group is weakened by strongly polar solvents, as such solvents partially deprotonate the acid, increasing its potential energy [42, 43]. Generally, UV spectra of sensitizers in solvents are reported. Therefore, we carried out our computational calculations assuming that the sensitizer was in a solvent. The reported UV spectrum in solvent also includes solvent effects that cause the absorption spectra to be slightly redshifted. This is quite consistent with the observations made in vibrational studies, and we expect that the selected architectural unit of the dye sensitizer will exhibit a high open circuit voltage.

In order to obtain information on the electronic transitions that occur in the dye, the corresponding MO properties were checked. The visible and near-UV regions are the most important regions for photocurrent conversion, so only the 19 lowest singlet/singlet transitions associated with absorption bands in the visible and near-UV regions for 2,3′-diamino-4,4′-stilbenedicarboxylic acid are listed in Table 5. The data shown in Table 5 and Fig. 7 were obtained using TD-DFT/6-311++G(d,p) with solvent effects included.

This indicates that the transitions are photoinduced charge-transfer processes, so the excitations generate charge-separated states, which should favor electron injection from the excited dye to the semiconductor surface.

The solar energy to electricity conversion efficiency (η) under AM 1.5 white-light irradiation can be obtained from the following formula:

$$\eta(\%) = \frac{J_{SC}[\mathrm{mAcm^{-2}}]V_{OC}[V]\mathrm{ff}}{I_0[\mathrm{mWcm^{-2}}]} \times 100,$$

where I_0 is the photon flux, J_{SC} is the short-circuit photocurrent density, V_{OC} is the open-circuit photovoltage, and ff represents the fill factor [44]. At present, J_{SC}, V_{OC}, and ff can only be obtained experimentally; the relationships between these quantities and the electronic structure of the dye are still unknown. We can calculate the open circuit voltage (V_{OC}) theoretically using the following expression [45] according to the sensitized mechanism (i.e., an electron is injected from the excited dye to the semiconductor conduction band):

$$V_{oc} = E_{HOMO}(\mathrm{donor}) - E_{LUMO}(\mathrm{acceptor}) - 0.3,$$

where E_{HOMO} is the energy of the organic dye molecule and E_{LUMO} is the energy of the semiconductor. Therefore, dyes with higher E_{HOMO} have larger V_{oc} values. However, this formula requires further verification through experimental study and theoretical calculations. J_{SC} is determined by two processes: the rate of electron injection from the excited dye to the conduction band of the semiconductor, and the rate of the redox reaction between the excited dye and the electrolyte.

The electrolyte has a very complex effect on the redox process, and this effect is not taken into account in the present calculations. This indicates that most of the excited states of 2,3′-diamino-4,4′-stilbenedicarboxylic acid have large absorption coefficients. With the short lifetimes of these excited states, the dye presents a high electron injection rate, which leads to the large J_{SC} value of 2,3′-diamino-4,4′-stilbenedicarboxylic acid. Based on the theoretical observations described above, it is clear that 2,3′-diamino-4,4′-stilbenedicarboxylic acid will exhibit enhanced performance compared to other sensitizers used in DSSCs. Further, this dye exhibits a large dipole moment in the excited state and high molecular polarizability, which leads to high photocurrent generation. Therefore, the results obtained in this study suggest that this selected dye architecture will exhibit good quantum efficiency.

Conclusions

For the first time, we have demonstrated a simple metal-free organic dye sensitizer that consists of an amino group acting as an electron donor and a carboxylic group acting as an electron acceptor, as well as a π-conjugated stilbene spacer between these groups. This type of structure leads to a high dipole moment, which greatly reduces dye recombination in its excited state and thus increases the efficiency of DSSCs that utilize this dye. The dye has a larger dipole moment in the excited state than in the ground state, and the difference in dipole moment between these states is comparable to the corresponding dipole moment differences for coumarin dyes. Indeed, this simple dye shows a larger dipole moment than more complex dye sensitizers, which suggests that using 2,3′-diamino-4,4′-stilbenedicarboxylic acid as a sensitizer in DSSCs will lead to improved photocurrent conversion efficiencies. Further, the results obtained in this study provide guidance on the optimal design of a simple D-π-A conjugated dye for use in DSSCs.

Acknowledgments One of the authors, Dr. C. Nithya, wishes to thank the Department of Science and Technology, India, for an INSPIRE Faculty Award.

References

1. O'Regan B, Gratzel M (1991) Nature 353:737–740
2. Gratzel M (2004) J Photochem Photobiol A 164:3–14
3. Nazeeruddin MK, Kay A, Rodicio L, Humphry-Baker R, Muller E, Liska P, Vlachopoulos N, Gratzel M (1993) J Am Chem Soc 115:6382–6390
4. Nazeeruddin MK, Pechy P, Renouard T, Zakeeruddin SM, Humphry-Baker R, Comte P, Liska P, Cevey L, Costa E, Shklover V, Spiccia L, Deacon GB, Bignozzi CA, Gratzel M (2001) J Am Chem Soc 123:1613–1624
5. Hara K, Sayama K, Ohga Y, Shinpo A, Suga S, Arakawa H (2001) Chem Commun 569–570
6. Wang ZS, Cui Y, Hara K, Dan-oh Y, Kasada C, Shinpo A (2007) Adv Mater 19:1138–1141
7. Horiuchi T, Miura H, Sumioka K, Uchida S (2004) J Am Chem Soc 126:12218–12219
8. Yang HY, Yen YS, Hsu YC, Chou HH, Lin JT (2010) Org Lett 12:16–19
9. Lin YD, Chow TJ (2011) J Mater Chem 21:14907–14916
10. Kim D, Lee JK, Kang SO, Ko J (2007) Tetrahedron 63:1913–1922
11. Tian Z, Huang M, Zhao B, Huang H, Feng X, Nie Y, Shen P, Tan S (2010) Dyes Pigm 87:181–187
12. Hwang S, Lee JH, Park C, Lee H, Kim C, Park C, Lee MH, Lee W, Park J, Kim K, Park NG, Kim C (2007) Chem Commun 4887–4889
13. Liang Y, Peng B, Chen J (2010) J Phys Chem C 114:10992–10998
14. Qin H, Wenger S, Xu M, Gao F, Jing X, Wang P, Zakeeruddin SM, Gratzel M (2008) J Am Chem Soc 130:9202–9203
15. Justin Thomas KR, Lin JT, Hsu YC, Ho KC, (2005) Chem Commun 4098–4100
16. Xia WS, Huang CH, Zhou DJ (1997) Langmuir 13:80–84
17. Lang AD, Zhai J, Huang CH (1998) J Phys Chem B 102:1424
18. Frisch MJ, Trucks GW, Schlegel HB, Scuseria GE, Robb MA, Cheeseman JR, Montgomery JA Jr, Vreven T, Kudin KN, Burant JC, Millam JM, Iyengar SS, Tomasi J, Barone V, Mennucci B, Cossi M, Scalmani G, Rega N, Petersson GA, Nakatsuji H, Hada M, Ehara M, Toyota K, Fukuda R, Hasegawa J, Ishida M, Nakajima T, Honda Y, Kitao O, Nakai H, Klene M, Li X, Knox JE, Hratchian HP, Cross JB, Adamo C, Jaramillo J, Gomperts R, Stratmann RE, Yazyev O, Austin AJ, Cammi R, Pomelli C, Ochterski JW, Ayala PY, Morokuma K, Voth GA, Salvador P, Dannenberg JJ, Zakrzewski VG, Dapprich S, Daniels AD, Strain MC, Farkas O, Malick DK, Rabuck AD, Raghavachari K, Foresman JB, Ortiz JV, Cui Q, Baboul AG, Clifford S, Cioslowski J, Stefanov BB, Liu G, Liashenko A, Piskorz P, Komaromi I, Martin RL, Fox DJ, Keith T, Al-Laham MA, Peng CY, Nanayakkara A, Challacombe M, Gill PMW, Johnson B, Chen W, Wong MW, Gonzalez C, Pople JA (2003) Gaussian 03. Gaussian, Inc., Pittsburgh
19. Becke AD (1993) J Chem Phys 98:5648–5652
20. Miehlich B, Savin A, Stoll H, Preuss H (1989) Chem Phys Lett 157:200–206
21. Lee C, Yang W, Parr RG (1988) Phys Rev B 37:785–789
22. Barone V, Cossi M (1998) J Phys Chem A 102:1995–2001
23. Cossi M, Rega N, Scalmani G, Barone V (2003) J Comput Chem 24:669–681
24. Nazeeruddin MK, De Angelis F, Fantacci S, Selloni A, Viscardi G, Liska P, Ito S, Takeru B, Gratzel M (2005) J Am Chem Soc 127:16835
25. Waston DF, Meyer GJ (2005) Annu Rev Phys Chem 56:119–156
26. Zhang W, Shi YR, Gan LB, Huang CH, Luo HX, Wu DG, Li NQ (1997) J Phys Chem B 103:675–681
27. Christiansen O, Gauss J, Stanton JF (1999) Chem Phys Lett 305:147–155
28. Dirk CW, Twing RJ, Wagniere G (1986) J Am Chem Soc 108:5397
29. Suppan P (1969) J Mol Spectrosc 30:17
30. Beens H, Knibbe H, Weller A (1967) J Chem Phys 47:1183
31. Kabatc J, Osmiałowski B, Paczkowski J (2006) Spectrochim Acta Part A 63:524–531
32. Sun Y, Chen X, Sun L, Guo X, Lu W (2003) Chem Phys Lett 381:397–403
33. Zhu X, Tsuji H, Yella A, Chauvin AS, Gratzel M, Nakamura E (2013) Chem Commun 49:582–584
34. Wong BM, Cardaro JG (2008) J Chem Phys 129:214703
35. Wu DG, Huang CH, Gan LB, Zhang W, Zheng J (1999) J Phys Chem B 103:4377–4381
36. Wang XF, Kitao Q (2012) Molecules 17:4484–4497
37. Merrick JP, Moran D, Radom L (2007) J Phys Chem A 111:11683–11700
38. Singa P, Boesch SE, Gu C, Wheeler RA, Willsom AK (2004) J Phys Chem A 108:9213–9217

39. Meic Z, Husten G (1978) Spectrochim Acta Part A 34:101–111
40. Panicker CY, Varghese HT, John A, Philip D, Istvan K, Keresztury G (2002) Spectrochim Acta Part A 58:281–287
41. Baranovic G, Meic Z, Maulitz AH (1998) Spectrochim Acta Part A 54:1017–1039
42. Wang ZS, Cui Y, Dan oh Y, Kasada C, Shinpo A, Hara K (2007) J Phys Chem C 111:7224–7230
43. Heredia D, Natera J, Gervaldo M, Otero L, Fungo F, Lin CY, Wong KT (2010) Org Lett 12:12–15
44. Hara K, Sato T, Katoh R, Furube A, Ohga Y, Shinpo A, Suga S, Sayama K, Sugihara H, Arakawa H (2003) J Phys Chem B 107:597–606
45. Belghiti N, Bennani M, Hamidi M, Bouzzine SM, Bouachrine M (2012) Afr J Pure Appl Chem 6:164–172